Frequency response and directivity of highly sensitive optical microresonator detectors for photoacoustic imaging

James A. Guggenheim, Jing Li, Edward Z. Zhang, and Paul C. Beard,

Department of Medical Physics and Biomedical Engineering, University College London, Gower Street, London WC1E 6BT, UK.

ABSTRACT

Plano-convex optical microresonator detectors have been developed as an alternative to planar Fabry-Pérot (FP) sensors used in all-optical photoacoustic imaging systems with the potential to provide two or more orders-of-magnitude higher detection sensitivity. This study further characterises the performance of these detectors by investigating their normal incidence frequency response and frequency-dependent directivity. It is shown that sensors with thicknesses in the range ~50-320μm provide broadband, smooth frequency response characteristics and low directional sensitivity. This suggests that a photoacoustic imaging system based on microresonator detectors may be capable of imaging with similar performance to the FP system but with significantly higher sensitivity, paving the way to deep tissue imaging applications such as the clinical assessment of breast cancer and preclinical whole body small animal imaging.

Keywords: photoacoustic imaging, Fabry-Pérot, NEP, frequency response, directivity, all-optical detection.

1. INTRODUCTION

The Fabry-Pérot (FP) sensor based photoacoustic imaging system [1] provides high-resolution photoacoustic imaging in tomography mode for depths up to ≈ 1cm [2]–[4] (figure 1). The transduction mechanism of the sensor is one in which an incident acoustic wave modulates its optical thickness resulting in a corresponding modulation in its reflectivity. The latter is then detected using a continuous wave interrogation laser beam focussed on the plane of the sensor.

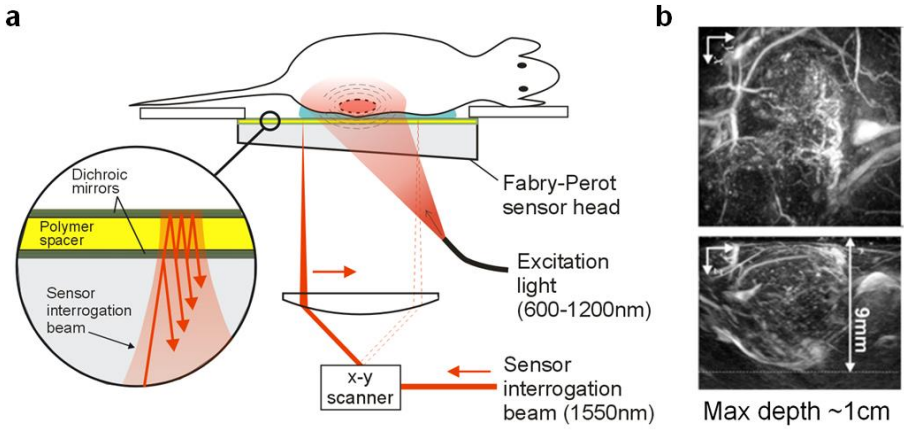

Figure 1: (a) Schematic and (b) sample image obtained with the planar Fabry-Pérot (FP) sensor based photoacoustic imaging system. The maximum penetration depth is ≈ **1**cm.

The sensitivity of the planar FP sensor is limited by the divergent nature of the interrogation beam which causes phase dispersion and beam walk-off thus limiting the practically achievable finesse and visibility (figure 2a). This in turn limits

Photons Plus Ultrasound: Imaging and Sensing 2015, edited by Alexander A. Oraevsky, Lihong V. Wang
Proc. of SPIE Vol. 9323, 93231C · © 2015 SPIE · CCC code: 1605-7422/15/$18
doi: 10.1117/12.2082514

the scope for increasing sensitivity either by increasing the FP mirror reflectances or spacer thickness (the latter with a cost in terms of bandwidth) [5]. To overcome this limitation, plano-convex optical microresonator sensors (figure 2b) have been developed [5]. These provide improved optical confinement thus allowing the finesse and therefore the sensitivity to be increased significantly. For example, NEPs (noise equivalent pressures) of 85Pa and 12Pa (over a 20MHz measurement bandwidth) have previously been reported for 50μm and 250μm thick prototype microresonators with -3dB bandwidths of 16MHz and 4MHz respectively [5]. By contrast, the sensitivity reported for a 50μm thick planar FP sensor with a 16MHz bandwidth was 370Pa [5]. This improvement in sensitivity offers the prospect of imaging to significantly greater depths than is currently achievable.

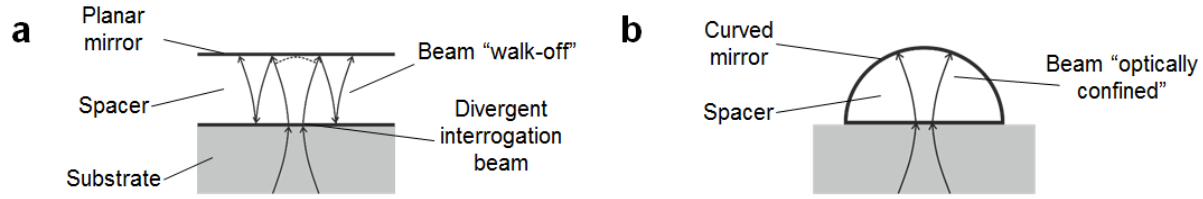

Figure 2: Schematics of (a) planar Fabry-Pérot and (b) plano-convex microresonator sensor interrogation illustrating beam walk-off in the planar sensor and its mitigation by using a plano-convex structure.

High sensitivity is not the only requirement of a photoacoustic detector however. A wideband frequency response is also required on account of the broadband nature of photoacoustic signals produced by pulsed excitation. Moreover, for tomography mode photoacoustic imaging, an omnidirectional response is required in order to detect photoacoustic waves over a large angular aperture. In this study, we extend the characterisation of these devices by measuring the normal-incidence frequency response and frequency-dependent directivity for a range of microresonator sensors with thicknesses spanning the range 48μm to 318μm.

2. METHODS

Sensor fabrication

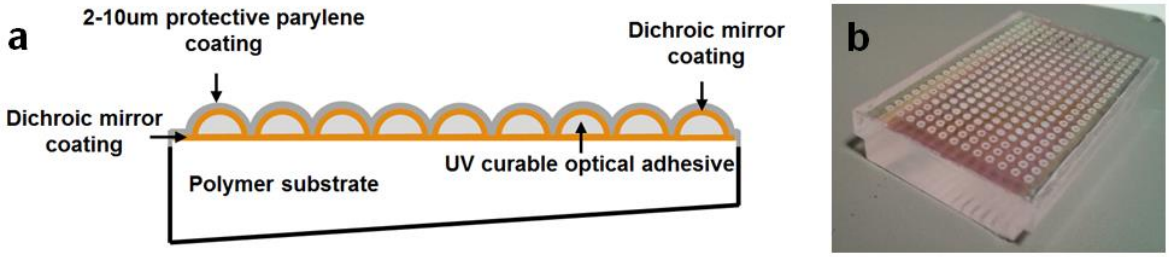

Figure 3: Schematic (a) and (b) photograph of a prototype microresonator sensor array

Figure 3 shows a schematic and photograph of a prototype microresonator sensor array. Plano-convex microresonator elements of different thicknesses were made by depositing controlled amounts of UV-curable optical adhesive onto mirror-coated polymer substrates using a precision microplotter. The deposited droplets were cured immediately using a UV gun. A second mirror was then deposited on to the cured polymer droplets followed by deposition of a protective Parylene C barrier coating.

Experimental set-up for measuring frequency response and directivity

Figure 4 shows the experimental set-up used for measuring frequency response and directivity. The sensors were mounted in a tank filled with olive oil and interrogated using an optical scanner. The acoustic source was a custom-built laser generated ultrasound source mounted on a PC-controlled rotating arm. The source comprised a 25mm diameter, 8mm thick PMMA disk coated on one side with highly absorbing black spray paint. The disk was illuminated by the output of a fibre-coupled Q-switched Nd:YAG laser emitting 10ns pulses at 1064nm. This resulted in the generation of planar acoustic waves with broadband frequency content in the range 1-70MHz. The rotating arm was first aligned such that its pivot point was coincident with the interrogation point on the microresonator of interest. For normal-incidence frequency response measurements the source was fixed at a distance of 7mm. For directivity measurements it was fixed at a distance of 4cm from the source and rotated in increments of 2° through angles of incidence of -50° to 50°. Signals were acquired and averaged over a number of laser pulses.

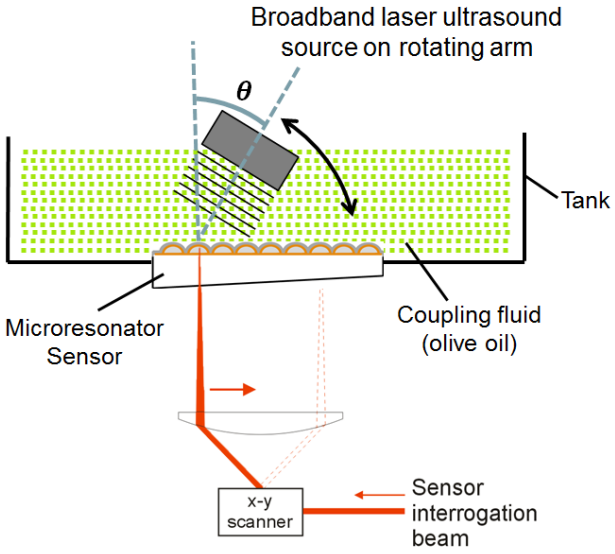

Figure 4: Experimental arrangement f**or** measuring frequency response and directivity

3. RESULTS AND DISCUSSION

Figures 5 and 6 show the normal-incidence frequency response and frequency-dependent directivity of a planar sensor of thickness 24μm and three microresonator sensors of thickness 48μm, 135μm, and 318μm. Measured data is plotted alongside simulated data obtained using established planar sensor models of frequency response[6] and directivity [7] for comparison. Each frequency response spectrum was corrected for the frequency spectrum of the acoustic source output which was measured using a 130MHz (-3dB bandwidth) planar FP sensor of known frequency response. Directivity results are shown for frequencies up to 11MHz because at higher frequencies the signal-to-noise ratio was poor owing to significant attenuation by the olive oil.

Figure 5(b) shows that the normal-incidence frequency response of the 24μm planar sensor is relatively flat for frequencies up to 25MHz. The directivity plots (figure 5c) show symmetrical response characteristics with respect to incident angle as expected. There is also qualitatively relatively good (though not perfect) agreement with the model data with features such as the sharp dips in sensitivity generally occurring at the correct angles – previous simulations of the directivity of a planar FP sensor [7] suggest that these minima may correspond to the critical angle for transmission of compressional and/or shear waves into the polymer. The normal-incidence frequency response of the 48μm microresonator (figure 5d-f) is well-matched with that of the planar sensor model. Its near uniform broadband frequency

response is consistent with the accompanying time-domain signal which exhibits little obvious distortion or ringing. The measured directivity is similar to that of the planar sensor in that it is generally relatively flat, symmetrical and broadly in agreement with the model for the studied range. An increased sensitivity to higher angles (beyond the first minimum predicted by the model) is evident, and in the measured data this appears higher than in the model, with maximum values near to +10dB. In general however, it can be seen that this detector exhibits low directional sensitivity between 0 and 50 degrees for the frequency range investigated.

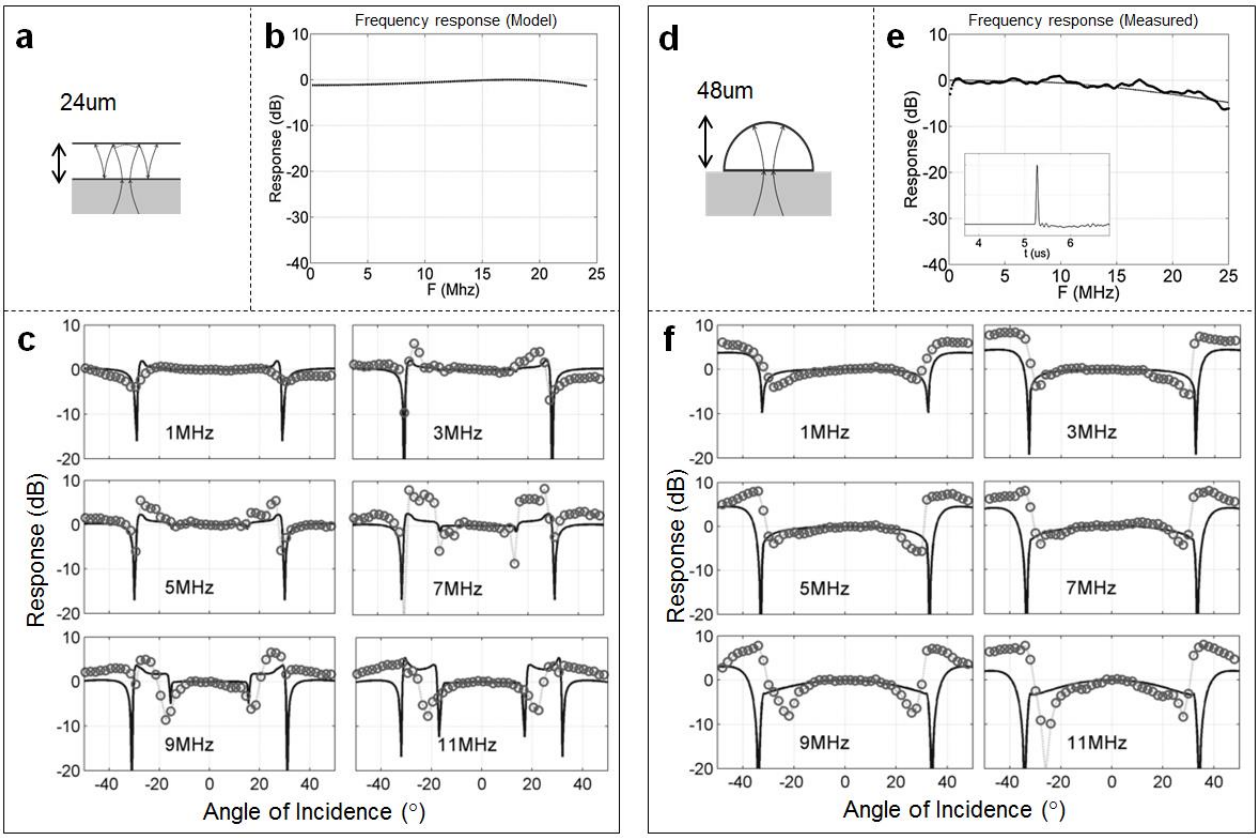

Figure 5: Frequency response and directivity of a 24µm thick planar sensor and a 48µm thick microresonator sensor. For these sensors respectively, the subfigures show (a, d) schematics (not-to-scale), (b, e) normal-incidence frequency response (with measured acoustic waveform where applicable), and (c, f) directional response plotted for a range of acoustic frequencies. On the normal-incidence frequency response plots, the grey dotted line shows simulated data obtained using an established planar sensor model [6] and the black dots show measured data. In the directivity plots the solid line shows data for a planar sensor [7] and the circles show measured data. For the 24µm planar sensor signals were averaged over 200 laser pulses when making directivity measurements. For the 48µm microresonator they were averaged over 1000 and 20 laser pulses for frequency response and directivity measurements respectively.

As shown in figure 6, the 135µm thick microresonator also has a normal-incidence frequency response in good agreement with the model. As expected, the increased thickness of this sensor compared to those in figure 5, results in a correspondingly reduced bandwidth with a smooth roll-off culminating in a minimum at approximately 18MHz. In terms of directivity, the results are similar to those of figure 5 in that there is a generally symmetrical, flat response, with an increased sensitivity at the highest studied angles. Again, there is reasonable agreement with the corresponding planar sensor model.

Unlike the 48µm and 135µm microresonators, the final microresonator presented, of thickness 318µm (figure 6d-f), was manufactured by laser cutting grooves into the substrate in order to spatially confine the liquid spacer material prior to curing. It was found that the time-domain signal for this and other sensors of various thicknesses produced in this way exhibited significant ringing as evident in the time-domain waveform (figure 6e). In order to estimate the normal-

incidence frequency response of this sensor without the influence of this effect, the first peak of the time-domain waveform was windowed out prior to computing its acoustic spectrum. Following this processing step, it appears from the frequency plot that the behaviour of the sensor is (other than for features introduced by the laser cutting) broadly in-line with expectations, i.e. a good match to the model is observed with several minima at expected locations. In the directivity plots (processed without windowing the main peak) the laser cutting does not appear to have had any obvious impact. As with the previous sensors the response appears relatively flat as a function of angle with an, albeit smaller, increase in sensitivity at the extremes of the measurement range and is in reasonable agreement with the planar sensor model.

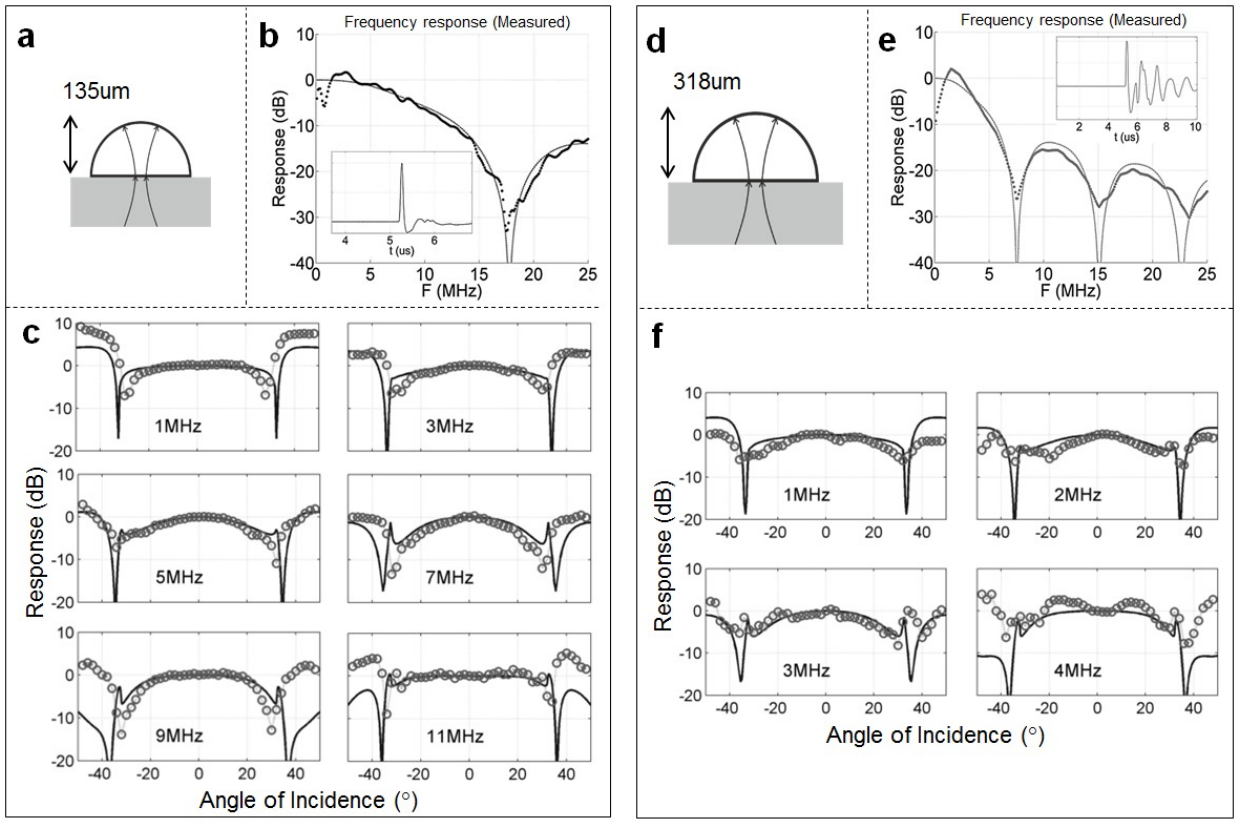

Figure 6: Characterisations of 135µm (a-c) and 318µm (d-f) microresonator sensors visualised as in figure 5. For the 135µm microresonator sensor signals were averaged over 200 and 40 laser pulses for frequency response and directivity measurements respectively. For the 318µm microresonator they were averaged over 160 and 40 laser pulses for frequency response and directivity measurements respectively.

4. CONCLUSIONS

Previous work [5] has shown that plano-convex microresonator sensors can provide significantly higher finesse and therefore higher sensitivity than the planar FP sensor. The current study has further characterised their performance by investigating their normal-incidence frequency response and frequency-dependent directivity. It was found that, in common with planar FP sensors, they provide a broadband, well-behaved frequency response and low directional sensitivity, both important requirements for photoacoustic imaging applications. An advantage of the concept is that it permits the development of a family of highly sensitive detectors with a range of bandwidths suitable for different applications. For example, the 48µm sensor (figure 5d-f) provides a -3dB bandwidth of 16MHz making it suitable for high resolution relatively superficial (<10mm) imaging. For deeper tissue imaging applications that require penetrations depths of several cm, the sensor thickness can be increased to achieve higher acoustic sensitivity: for example it has previously been reported that a 250µm thick microresonator sensor with a -3dB bandwidth of 4MHz can provide an NEP

of 12Pa (over a 20MHz measurement bandwidth) [5]. Although increasing the sensor thickness reduces the bandwidth, this is not necessarily prohibitive for deep tissue imaging due to the significant bandlimiting of the photoacoustic signal by frequency dependent acoustic attenuation in tissue. The results obtained in this study suggests that this new type sensor has the potential to provide images of similarly high quality as those obtained with the FP planar sensor but at greater depths thereby paving the way to deep tissue imaging applications such as the assessment of tumours in the breast and whole body small animal imaging.

ACKNOWLEDGMENTS

The authors acknowledge support from EPSRC and European Union project FAMOS (FP7 ICT, Contract 317744). Technical support concerning fabrication using the microplotter was provided by Steve Hudziak.

REFERENCES

[1] E. Zhang, J. Laufer, and P. Beard, "Backward-mode multiwavelength photoacoustic scanner using a planar Fabry-Perot polymer film ultrasound sensor for high-resolution three-dimensional imaging of biological tissues," *Appl. Opt.*, vol. 47, no. 4, pp. 561–77, Feb. 2008.

[2] J. Laufer, F. Norris, J. Cleary, E. Zhang, B. Treeby, B. Cox, P. Johnson, P. Scambler, M. Lythgoe, and P. Beard, "In vivo photoacoustic imaging of mouse embryos," *J. Biomed. Opt.*, vol. 17, no. 6, p. 061220, 2012.

[3] E. Z. Zhang, J. G. Laufer, R. B. Pedley, and P. C. Beard, "In vivo high-resolution 3D photoacoustic imaging of superficial vascular anatomy," *Phys. Med. Biol.*, vol. 54, no. 4, pp. 1035–46, Feb. 2009.

[4] J. Laufer, P. Johnson, E. Zhang, B. Treeby, B. Cox, B. Pedley, and P. Beard, "In vivo preclinical photoacoustic imaging of tumor vasculature development and therapy," *J. Biomed. Opt.*, vol. 17, no. 5, pp. 056016–1 – 056016–8, May 2012.

[5] J. Li, A. Taylor, I. Papakonstantinou, E. Zhang, and P. Beard, "Highly sensitive optical microresonator sensors for photoacoustic imaging," in *Proceedings of SPIE*, 2014, vol. 8943, pp. 89430C–1 – 89430C–10.

[6] P. C. Beard, F. Perennes, and T. N. Mills, "Transduction mechanisms of the Fabry-Perot polymer film sensing concept for wideband ultrasound detection," *IEEE Trans. Ultrason. Ferroelectr. Freq. Control*, vol. 46, no. 6, pp. 1575–1582, Jan. 1999.

[7] B. T. Cox and P. C. Beard, "The frequency-dependent directivity of a planar fabry-perot polymer film ultrasound sensor.," *IEEE Trans. Ultrason. Ferroelectr. Freq. Control*, vol. 54, no. 2, pp. 394–404, Feb. 2007.